Inorganica Chimica Acta 374 (2011) 334–340

Contents lists available at ScienceDirect

Inorganica Chimica Acta

journal homepage: www.elsevier.com/locate/ica

Exploring the properties of mixed valence cyanide bridged dinuclear complexes: Solvent stabilization of electronic isomers

Melina B. Rossi, Pablo Alborés, Luis M. Baraldo *

Departamento de Química Analítica, Inorgánica y Química Física, Facultad de Ciencias Exactas y Naturales, Universidad de Buenos Aires, INQUIMAE, CONICET, Pabellón 2, Ciudad Universitaria, C1428EHA Buenos Aires, Argentina

ARTICLE INFO

Article history:
Available online 13 March 2011

Dedicated to Prof. W. Kaim

Keywords:
Cyanide bridged complexes
Metal–metal interaction
Mixed valence complexes
Intervalence charge transfer
Solvent effect
Spectroelectrochemistry

ABSTRACT

We report here the synthesis and properties of a family of mixed-valence cyanide-bridged dinuclear complex ions *trans*-$[(L'L_4Ru^{II}(\mu\text{-NC})Fe^{III}(CN)_5]^-$ (with L = pyridine or 4-dimethylaminopyridine (dmap) and L′ = pyridine, 4-methoxypyridine (meopy) or 4-dimethylaminopyridine)) whose properties could be adjusted smoothly by changing the acceptor properties of the solvent and the σ donor properties of the L′ pyridine ligand. In solution these complexes exhibit an intense solvent-dependent MM′CT ($Ru^{II} \rightarrow Fe^{III}$) absorption in the near infrared region. Analysis of this band in different complexes and solvents suggests an enhanced interaction as the energies of the metal centers come closer. From this trend the anion *trans*-$[(dmap)_5Ru(\mu\text{-NC})Fe(CN)_5]^-$ (dmap = 4-dimethylaminopyridine) in water is expected to belong to the class II-III, but its spectral properties indicates a ground state with Ru(III)–Fe(II) character. The stabilization of this electronic isomer is probably related to the better donor properties of the hexacyanoferrate(II) moiety and its stronger interaction with water.

1. Introduction

Mixed valence chemistry has attracted the attention of chemist for several decades [1] mainly due to its intimate connection with the rationalization of electron transfer processes. Recently one of the topics of interest has been the properties of systems in the boundary between class II (weakly interacting) and class III (delocalized) [2]. A new class II–III has been proposed, where the electron distribution is non-symmetrical in the short time scale, but moving fast enough that it results averaged in the time scale of the reorganization of the solvent [3].

Cyanide is probably the non-symmetrical bridge most extensively investigated in mixed-valence chemistry [4–15], and most of the explored systems have been classified as belonging to class II. Recently we have reported the properties of a cyanide-bridged trinuclear complex, *trans*-$[(dmap)_4Ru\{(\mu\text{-NC})Os(CN)_5\}_2]^{4-}$, that is beyond the class II and presents evidence of partial redox states for the three metal ions [16]. Encouraged by this result, we set to explore a new family of mixed valence dinuclear anions, *trans*-$[(L'L_4Ru^{II}(\mu\text{-NC})Fe^{III}(CN)_5]^-$ (Scheme 1) whose properties could be adjusted smoothly by changing the acceptor properties of the solvent and the σ donor properties of the L′ pyridine ligand. In order to level the donor and acceptor energies, the replacement of a L pyridine ligand by a dmap ligand is a step foward, as it lowers the ruthenium redox potential by ~0.15 V, bringing it closer to the redox potential of hexacyanoferrate in water. We also present the properties of *trans*-$[(dmap)_5Ru^{II}(\mu\text{-NC})Co^{III}(CN)_5]^-$, which is a useful diamagnetic reference system for this family of compounds. Scheme 1 presents the chemical structures of the complexes reported in this work.

2. Experimental

2.1. Materials

The complexes $[Ru(dmap)_6]Cl_2{\cdot}9H_2O$ [17] and *trans*-$[(L)Ru^{II}(py)_4Cl](PF_6)$ [18] were prepared following previously described. $(Ph_4P)_3[Fe(CN)_6]{\cdot}2H_2O$ (Ph_4P^+ = tetraphenylphosphonium) was prepared by addition of solid $(Ph_4P)Cl$ to an aqueous solution of $K_3[Fe(CN)_6]$, followed by filtration, washing with cold water and vacuum drying. Solvents for UV–Vis–NIR and electrochemistry measurements were dried according to literature procedures [19]. All other reagents were obtained commercially and used as supplied. The compounds synthesized in this work were dried in a vacuum desiccator for at least 12 h prior to characterization.

2.2. Synthesis of the complexes

2.2.1. *trans*-$[(L)Ru^{II}(py)_4(\mu\text{-NC})Fe^{III}(NC)_5](TPP)$

([**1**](TPP), L = py, [**3**](TPP), L = dmap) and *trans*-$[(meopy)Ru^{II}(py)_4(\mu\text{-NC})Fe^{III}(NC)_5](PNP)$, ([**2**](PNP)), PNP^+ = bis(triphenylphosphine)iminium). $[(L)Ru^{II}(py)_4Cl](PF_6)$ (*ca.* 300 mg, 0.44 mmol) was

* Corresponding author. Tel.: +54 11 4576 3380; fax: +54 11 4576 3341.
E-mail address: baraldo@qi.fcen.uba.ar (L.M. Baraldo).

0020-1693/$ - see front matter © 2011 Elsevier B.V. All rights reserved.
doi:10.1016/j.ica.2011.03.032

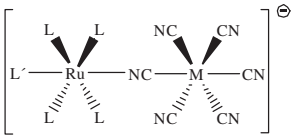

Complex	M	L	L´
1	Fe	py	py
2	Fe	py	meopy
3	Fe	py	dmap
4	Fe	dmap	dmap
5	Co	dmap	dmap

Scheme 1. Anions reported in this work (py = pyridine, meopy = 4-methoxypyridine, dmap = 4-dimethylaminopyridine).

suspended in 50 ml of methanol and treated with a solution of (175 mg, 0.53 mmol) $K_3Fe(CN)_6{\cdot}3H_2O$ in 50 ml of water. The mixture was stirred and heated at different temperatures, according to the identity of the *trans* ligand ((**1**): $T = 40$ °C; (**2**): $T = 35$ °C and (**3**): $T = 25$ °C), in the dark for 2 h. The resulting green solution was filtered to remove a small amount of unreacted ruthenium precursor and then evaporated to dryness. The solid residue was extracted with methanol to eliminate the excess of potassium hexacyanoferrate(III) and the clear green solution was evaporated to dryness. The green solid was dissolved in a minimum amount of water and treated with solid $(Ph_4P)Cl$ or (PNP)Cl. The pale green precipitate was collected by filtration, washed several times with water and vacuum dried.

Purification was performed by exclusion chromatography using a Sephadex LH-20 column, packed and eluted with methanol. The second colored fraction, which contained the desired product, was collected and evaporated to dryness; the resulting green solid was dried under vacuum. Further purification was achieved by recrystalization from methanol/ether. Yields ranged between 30% and 34%, depending on the anion. *Anal.* Calc. for ([**1**](TPP)·6 H_2O): $C_{55}H_{57}N_{11}O_6PFeRu$: C, 57.1; H, 4.9; N, 13.3. Found: C, 56.8; H, 4.6; N, 13.3%. IR ν (CN): 2109 cm^{-1}(s); *Anal.* Calc. for ([**2**](PNP)·1H_2O): $C_{68}H_{59}N_{12}O_2P_2FeRu$: C, 58.9; H, 4.3; N, 14.7. Found: C, 58.3; H, 4.2; N, 14.7%. IR ν (CN): 2110 cm^{-1}(s); *Anal.* Calc. for ([**3**](TPP)·5H_2O): $C_{57}H_{64}N_{12}O_7PFeRu$: C, 55.4; H, 4.9; N, 13.6. Found: C, 55.7; H, 4.8; N, 14.0%. ν(CN): 2110 cm^{-1}(s).

trans-$[(dmap)_5Ru^{II}(\mu\text{-}NC)M^{III}(NC)_5](Ph_4P)\cdot 6H_2O$ ([**4**](TPP)·6H_2O, M = Fe and ([**5**](TPP).5.5H_2O, M = Co) $[Ru^{III}(dmap)_5(OH)]Cl_2$ (300 mg, 0.34 mmol) was dissolved in 7 ml of ethanol, reduced with solid ascorbic acid and treated with $(Ph_4P)_3[M(CN)_6]{\cdot}2H_2O$ (M: Fe, 463 mg, 0.37 mmol; M: Co, 469 mg, 0.37 mmol) in 7 ml of ethanol. The resulting mixture was stirred at 25 °C in the dark for 15 min. A green precipitate was collected by filtration, washed with ethanol and vacuum dried (yield: 243 mg (46%)). *Anal.* Calc. for $C_{65}H_{82}N_{16}O_6PFeRu$: C, 56.9; H, 6.0; N, 16.3. Found: C, 57.3; H, 6.0; N, 16.4%. ν(CN): 2108 cm^{-1}(s). *Anal.* Calc. for $C_{65}H_{81}N_{16}O_{5.5}PRuCo$: C, 56.8; H, 6.0; N, 16.3. Found: C, 56.5; H, 5.8; N, 17.0%. ν(CN): 2116 cm^{-1}(s). δ_H (CD_3OD) 8.92 (2, d, H^1 py. ax.), 8.81 (8, d, H^1 py. eq.), 7.64 (2, d, H^2 py. ax.), 7.52 (8, d, H^2 py. eq.), 4.02 (24, s, H^{CH3} py. eq.), 2.96 (6, s, H^{CH3} py. ax.).

2.2.2. trans-$[(L'L_4Ru^{II}(\mu\text{-}NC)Fe^{III}(CN)_5]Na{\cdot}xH_2O$

trans-$[(L'L_4Ru^{II}(\mu\text{-}NC)Fe^{III}(CN)_5](TFF){\cdot}xH_2O$ (0.1 g) was dissolved in a minimum volume of acetonitrile and 0.01 g of $NaClO_4$ were added. The resulting solution is stirred until a light colored precipitate is observed (**1** and **2** green, **4** blue). The solid is collected by filtration, washed with acetonitrile and dichloromethane and dried under vacuum. Yield. 55–60%. (**1**Na·6H_2O) *Anal.* Calc. for $C_{31}H_{37}N_{11}O_6FeRuNa$: C, 44.3; H, 4.4; N, 18.4. Found: C, 44.2; H, 4.5; N, 17.9%. ν(CN): 2109 cm^{-1} (s). (**2**Na·1H_2O) *Anal.* Calc. for $C_{32}H_{29}N_{11}O_2FeRuNa$: C, 49.4; H, 3.6; N, 19.8. Found: C, 48.7; H, 4.1; N, 19.8%. ν(CN): 2108 cm^{-1} (s). (**4**Na·6H_2O) *Anal.* Calc. $C_{41}H_{62}N_{16}O_6FeRuNa$: C, 46.7; H, 5.9; N, 21.3. Found: C, 45.8; H, 6.4; N, 20.5%. ν(CN): 2054 cm^{-1} (s).

2.3. Physical measurements

IR spectra were collected with a Nicolet FTIR 510P instrument, using KBr pellets or solutions employing CaF_2 windows of 3 cm ∅ and a 0.05 mm Teflon spacer. UV–Vis spectra were recorded with a Hewlett–Packard 8453 diode array spectrophotometer in the range between 190 and 1100 nm or with a Shimadzu 3100 UV–Vis/NIR for the NIR region (up to 2500 nm). Elemental analyses were performed with a Carlo Erba 1108 analyzer. Hydration water molecules in the reported complexes were determined by thermogravimetric measurements with a TGA-51 Shimadzu thermogravimetric analyzer. NMR spectra were obtained with a Bruker AM-500 spectrometer. Cyclic voltammetry measurements were carried out with millimolar solutions of the compounds, using a TQ3 potentiostat and a standard three electrode arrangement consisting of a glassy carbon disk (area = 9.4 mm^2) as the working electrode, a platinum wire as the counter electrode and a reference electrode. The latter was a silver wire plus an internal ferrocene (F_c) standard. Tetra-*N*-butylammonium-hexafluorophosphate ($TBAPF_6$) 0.1 M was used as supporting electrolyte. All potentials reported in this work are referenced to the standard AgCl/Ag saturated KCl electrode (0.197 V versus NHE), using the accepted values for the F_c^+/F_c couple in different media [20]. Infrared and UV–vis–NIR spectroelectrochemical measurements were performed with an optically transparent thin layer electrode (OTTLE) cell [21], equipped with two 40 × 20 mm CaF_2 windows (with about 0.20 cm of path length), a working Pt electrode grid (0.25 mm^2), a Pt counter electrode grid (0.50 mm^2), and an Ag wire reference electrode.

3. Results and discussion

3.1. Synthesis

We have prepared two new members of the previously reported family of ruthenium complexes *trans*-$[(L)(py)_4Ru^{II}Cl]^+$ [18] incorporating the more basic pyridine ligands 4-methoxypyridine and 4-dimethylaminopyridine. The rationale behind our ligand choice was to have ruthenium fragments with a redox potential closer to the one observed for the hexacyanoferrate moiety in water. A dinuclear compound showing similar redox potentials for both centers would be a good candidate to show some degree of electronic delocalization between the metals. The reaction of *trans*-$[(L)(py)_4Ru^{II}Cl]^+$ complexes with $K_3([Fe(CN)_6]$ in a methanol/water solution at moderate temperature results in the formation of the dinuclear complex $[(L)(py)_4Ru^{II}(\mu\text{-}NC)Fe^{III}(CN)_5]^-$. These anions were easily precipitated from water solution as the PPh_4^+ salt and further purification was achieved from size exclusion chromatography in methanol. Temperature control is required to avoid the formation of the trinuclear complex *trans*-$[(py)_4Ru\{(\mu\text{-}NC)\text{-}Fe(CN)_5\}_2]^{4-}$ [15] When L is dmap, the resulting complex is less inert and hence a lower temperature of reaction is required to avoid the formation of byproducts.

A redox couple with even lower redox potential can be achieved by the incorporation of five dmap ligands in the coordination sphere of the ruthenium. We have recently reported the

preparation of $[Ru(dmap)_6]Cl_2{\cdot}9H_2O$, [17] which reacts in aerated water to afford $[Ru(dmap)_5(OH)]^{2+}$, a useful starting material to prepare $[Ru(dmpa)_5L]^{n+}$ complexes. It also reacts at room temperature in ethanol with the tetraphenyphosphonium (PPh_4^+) salt of different hexacyanometallates(III) (Fe and Co) to yield an analytically pure dinuclear compound of formula $[PPh_4^+][(dmap)_5Ru^{II}(\mu\text{-}NC)M^{III}(CN)_5]$. In the case of the diamagnetic dinuclear ion $[(dmap)_5Ru^{II}(\mu\text{-}NC)Co^{III}(CN)_5]^-$, the ^1H NMR confirms the proposed structure.

3.2. Electrochemistry

Cyclic voltammograms of the five reported dinuclear complexes in methanol are shown in Fig. 1, while the relevant electrochemical data is presented in Fig. 2 and Table 1.

Two reversible one electron processes are observed for **1–4**, while **5** presents one reversible process and an irreversible reduction wave at very low potential, compatible with the replacement of iron by cobalt in the hexacyanide moiety. The potential of the reversible anodic wave, corresponding to a $Ru^{II} \rightarrow Ru^{III}$ process, depends mainly on the coordination sphere of ruthenium; being higher for anion **1,** where the ruthenium is surrounded by five

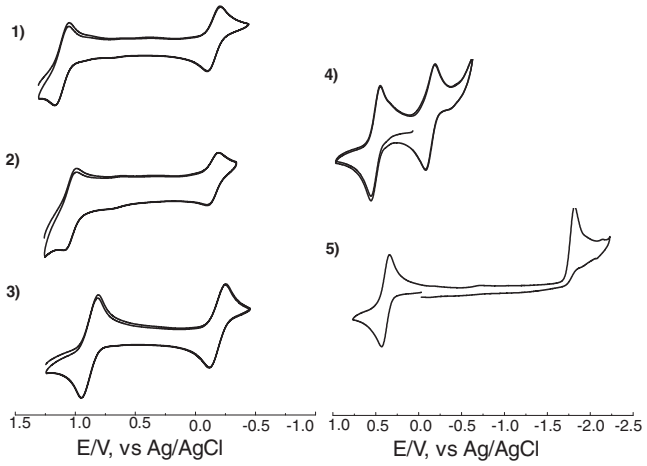

Fig. 1. Cyclic voltammograms in methanol for complexes **1**, **2**, **3**, **4** and **5**.

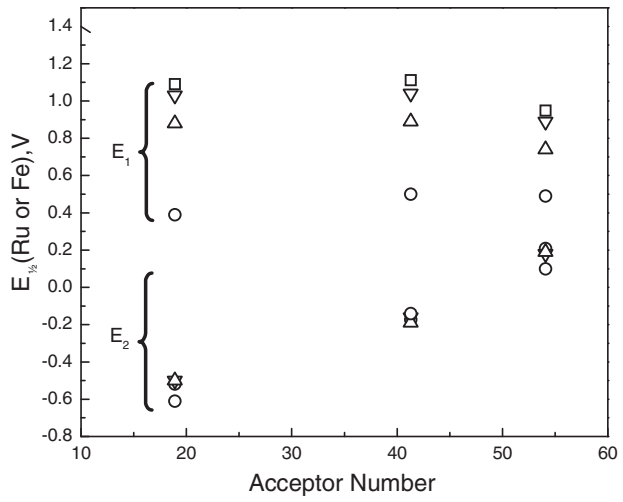

Fig. 2. Correlation between the two redox potentials for the reported dinuclear compounds **1** (□), **2** (Δ), **3**(Δ) and **4** (○) and the acceptor number of the solvent. E_1 refers to the anodic wave (usually Ru) and E_2 refers to the cathodic wave (usually Fe).

Table 1
Redox potential for the Ru(III)/(II) and Fe(III)/(II) couples of the dinuclear compounds **1–5** in different solvents.

Complex	Solvent	$E_{1/2}$(Ru)/V (ΔE_p/mV)	$E_{1/2}$(Fe)/V (ΔE_p/mV)	$E_{1/2}$(Co)/V (ΔE_p/mV)	ΔE_{Ru-Fe}/V
1	acetonitrile	1.09 (87)	−0.52 (115)	–	1.61
	methanol	1.11 (115)	−0.17 (106)	–	1.28
	water	0.95 (69)	0.21 (71)	–	0.74
2	acetonitrile	1.03 (96)	−0.50 (91)	–	1.53
	methanol	1.04 (97)	−0.16 (84)	–	1.20
	water	0.89 (88)	0.18 (78)	–	0.71
3	acetonitrile	0.88 (107)	−0.50 (105)	–	1.38
	methanol	0.89 (141)	−0.19 (135)	–	1.08
	water	0.74 (69)	0.19 (94)	–	0.55
4	acetonitrile	0.39 (119)	−0.61 (137)	–	1.00
	methanol	0.50 (107)	−0.14 (95)	–	0.64
	water	0.10 (104)	0.49 (112)	–	0.39
5	acetonitrile	0.38 (95)	–	−1.81 (irrev.)	–
	methanol	0.32 (107)	–	−1.75 (irrev.)	–

pyridine ligands, the less basic ligand of the set. There is only a very moderate solvent effect on the $E_{½}$ of these couples, but the potentials of the reduction wave, corresponding to the Fe^{III}/Fe^{II} couple, are strongly solvent dependent instead. Fig. 2 shows the linear correlation of the redox potential of this couple with the Gutmann acceptor number of the solvent for the different complexes reported in this work. A similar dependence has been observed for other cyanocomplexes [13,15,22]. As observed in Fig. 2, the smaller $\Delta E_{½Ru-Fe}$ corresponds to the *trans*-$[(dmap)_5Ru^{II}(\mu\text{-}NC)Fe^{III}(CN)_5]^-$ (**4**) in water, even though in this case the assignment of the redox couples is not straightforward (see below).

3.3. Spectroscopic Properties of mixed valence ions

In all the solvents explored, complexes **1–5** exhibit the electronic spectroscopic features expected for a ruthenium polypyridine; a intense band in the vis region, corresponding to a $Ru^{II} \rightarrow \pi^*$ (pyridine ligand) MLCT transition (Fig. 3 and Table 2). The exception to this behavior is the spectrum of complex **4** in water (Fig. 5). For complexes with more than one type of pyridine ligand, overlapping bands are observed. In addition, compounds **1–4** present another band in the Vis–NIR region that corresponds to the $Ru^{II} \rightarrow Fe^{III}$ MM′CT transition. The energy of this MM′CT band correlates with the difference in the redox potential between the iron and the ruthenium centers (Fig. 3), confirming its nature.

The transition moment (which reflects the true integrated intensity) of the MM′CT band of this family of complexes in different solvents correlates well with the energy of the transition (Fig. 4a) as observed for the ions in the *trans*-$[L_4Ru\{(\mu\text{-}NC)\text{-}Fe(CN)_5\}_2]^{4-}$ family [15]. This result is usually not observed as different solvents would have different contributions to the reorganization energy. However in this case, the specific donor/acceptor interaction of the solvent with the terminal cyanides not only affects the energy of the acceptor site (and, as a consequence, the difference of energy between the donor/acceptor sites and hence the mixing between them, which results in a larger transition moment for the MM′CT), but also the reorganization energy of the MM′CT transition. In this case, the specific interaction of the terminal cyanides with the solvent is even stronger in the excited state of this transition than in the ground state, as the former has a $Fe^{II}(CN)_5$ fragment which is a better donor than the $Fe^{III}(CN)_5$ moiety. As a result, a stabilization of the excited state should be operative. In fact, this seems to be the case, as the extrapolation of the MM′CT energy at $\Delta E_{½Ru-Fe} = 0$ (Fig. 3b) gives a low value of only $2700 \pm 400\ cm^{-1}$.

The energy of the MM′CT transition also depends on the acceptor number of the solvent. Fig. 4b shows this correlation for the

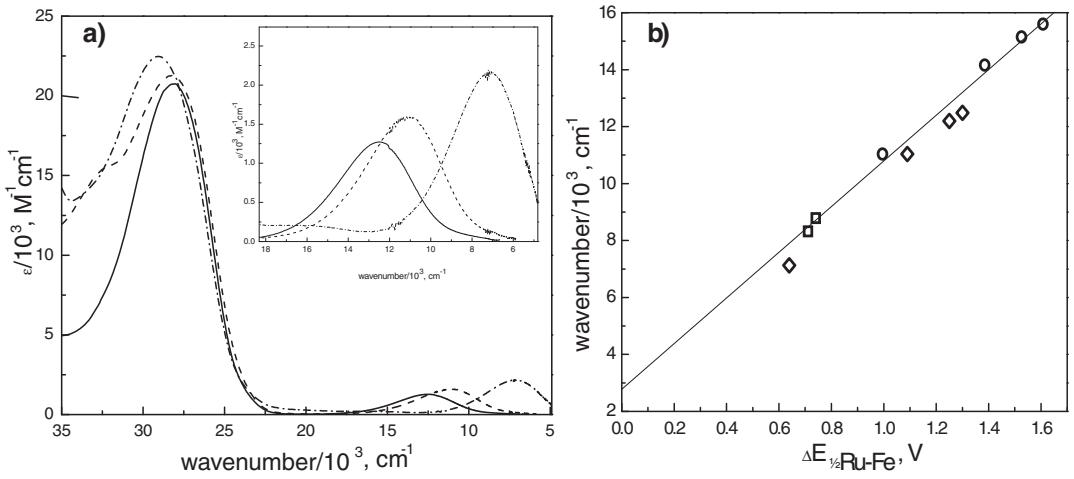

Fig. 3. (a) Vis–NIR spectra of complexes **1** (–), **3** (– –) and **4** (– · –) in methanol; (b) correlation between the MM′CT energy and $\Delta E_{½Ru-Fe} = E_{½}(Ru(III/II)) - E_{½}(Fe(III/II))$ for species **1**–**4** in acetonitrile (○), methanol (◇) and water (□).

Table 2
UV–Vis–NIR properties of compounds **1**–**5** in different solvents.

Complex	Solvent	MLCT $\nu/10^3$ cm^{-1} ($\varepsilon/10^3$ M^{-1} cm^{-1})	LMCT $\nu/10^3$ cm^{-1} (ε/M^{-1} cm^{-1})	MM′CT $\nu/10^3$ cm^{-1} ($\varepsilon/10^3$ M^{-1} cm^{-1})
1	dimethylacetamide	27.0 (24.2)		17.0 (0.7)15.6 (0.9)13.7 (1.0)12.5 (1.4) 8.8 (2.8)
	acetonitrile	27.7 (24.1)		
	ethanol	27.9 (19.1)		
	methanol	28.1 (22.8)		
	water	28.7 (22.6)		
2	dimethylacetamide	27.2 (15.2)		16.7 (0.5)15.2 (0.7)13.2 (1.0)12.2 (1.2)8.3 (2.3)
	acetonitrile	27.7 (18.0)		
	ethanol	27.9 (18.6)		
	methanol	28.1 (18.0)		
	water	28.7 (16.4)		
3	dimethylacetamide	27.1 (22.7)/31.5(14.0)		15.8 (0.7)14.2 (1.0)12.3 (1.4)11.0 (1.4)
	acetonitrile	27.7 (23.5)/32.1(15.7)		
	ethanol	27.9 (23.0)/32.3 (15.5)		
	methanol	28.2 (17.7)/32.2(15.2)		
4	dimethylacetamide	27.8 (20.3)		12.4 (0.7)
	acetonitrile	28.2 (20.0)		11.0 (0.9)
	methanol	29.1 (21.4)		7.2 (2.2)
	water	–	7.2 (4.3)/15.2 (5.4)	6.1 (4.8)
5	acetonitrile	27.4 (22.2)		
	methanol	28.7 (28.8)		

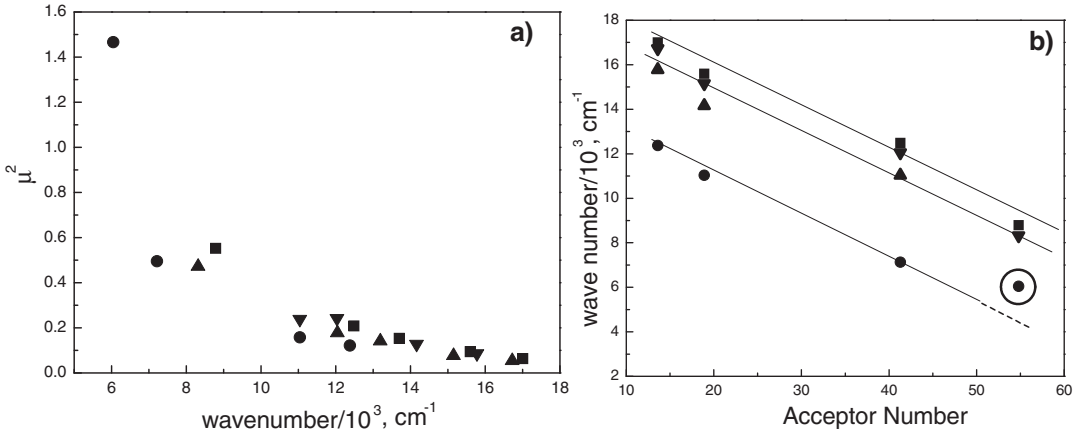

Fig. 4. (a) Transition moment of the MM′CT transition as a function of its energy: 1(■), 2 (▲), 3 (▼) and 4 (●); (b) Correlation of the energy of the MM′CT transition with the acceptor number of the solvent. In the latter, the circle shows that the energy of the MM′CT transition for compound **4**, in water, is higher than the expected value, according to the observed trend.

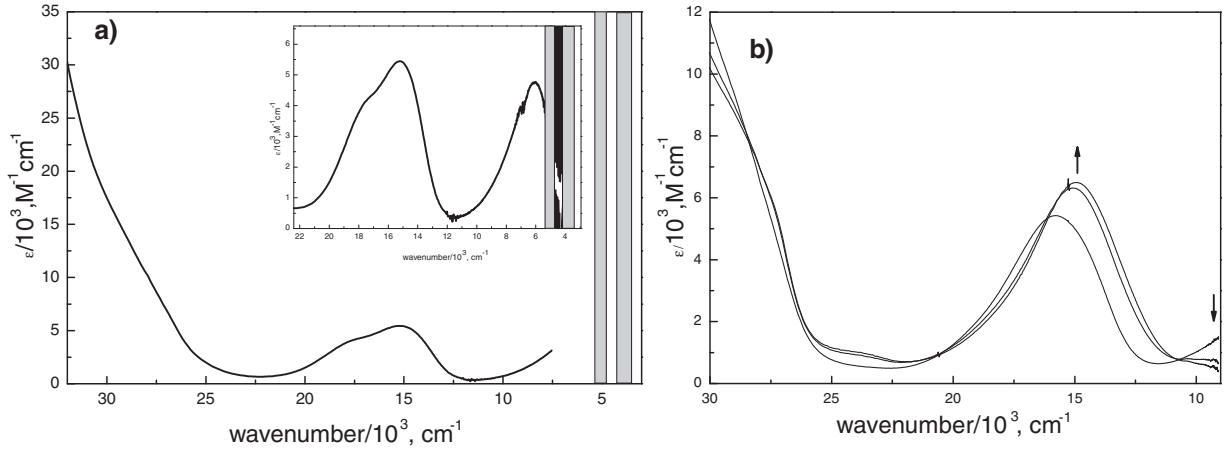

Fig. 5. (a) Vis–NIR spectrum of complex **4** in water, the inset shows a detail of the LMCT band; (b) oxidation of **4** in water, the spectra shows the shift of the LMCT transition to lower energies and the decline of the MM′CT band.

complexes **1–4**. From this correlation it is clear that the value observed for complex **4** in water is much higher than the 4000 cm^{-1} value expected from the observed trend.

Turning our attention to the atypical spectrum of **4** in water (Fig. 5), two distinct features are clear; the intense MLCT band around 28×10^3 cm^{-1} is missing and new bands at 15.2 and 17.2×10^3 cm^{-1} are observed. These new bands are probably LMCT transitions from the filled π orbitals of the dmap to a vacant dπ orbital of the Ru(III) ion. Similar transitions have been observed for other Ru^{III}dmap complexes [17,23,24] and they are also present in the oxidized form of **4**, slightly displaced to lower energies (Fig. 5b). This evidence suggest that the configuration of **4** in water is Ru(III)–Fe(II) instead of the Ru(II)–Fe(III) isomer, so in this case, the Ru^{III}/Ru^{II} redox couple occurs at lower potential than the Fe^{III}/Fe^{II} process. It is worthy to mention that a similar ordering of the redox potentials have been observed for the related dinuclear anion $[(NH_3)_5Ru^{III}(\mu\text{-}NC)Fe^{II}(CN)_5]^-$ in water [25]. The band at 6.1×10^3 cm^{-1} is also a MM′CT transition, but from the Fe(II) to the Ru(III).

3.4. Infrared spectroscopy

In order to explore the donor acceptor coupling properties of these dinuclear complexes and to identify the nature of electronic isomer present, we also explored the IR spectra of this family of complexes in solution. Most of the systems show absorptions around 2100 cm^{-1}, which correspond to overlapping bands of the ν_{CN} stretching modes of the coordinated cyanide ligands in the hexacyanometallate(III). The energy of these bands is slightly displaced to lower energies in the presence of less acceptor solvents or better donor ligands.

In methanol, another band can be observed at lower energies. It is barely distinguishable for complex **1** (Fig. 6a), but very intense and broad for complex **4** (Fig. 6b). This band is only present in the mixed valence form of **4** and it is absent in its oxidized and reduced form (Fig. S1). We assign it as the ν_{CN} band corresponding to the bridging cyanide. The literature contains several reports of ν_{CN} of bridging cyanides that are displaced to lower energies when there is a significant interaction between the dπ orbitals of the bridged moieties and the π* of the cyanide bridge [6,8,9,26–30]. The same phenomenon has also been observed for the bridging moieties in other mixed valence systems [31] and usually they are also very intense and broad. This intensification goes beyond what is expected for a polar moiety and entanglement between vibrational and electronic states has been suggested as the possible origin of this phenomenon [9].

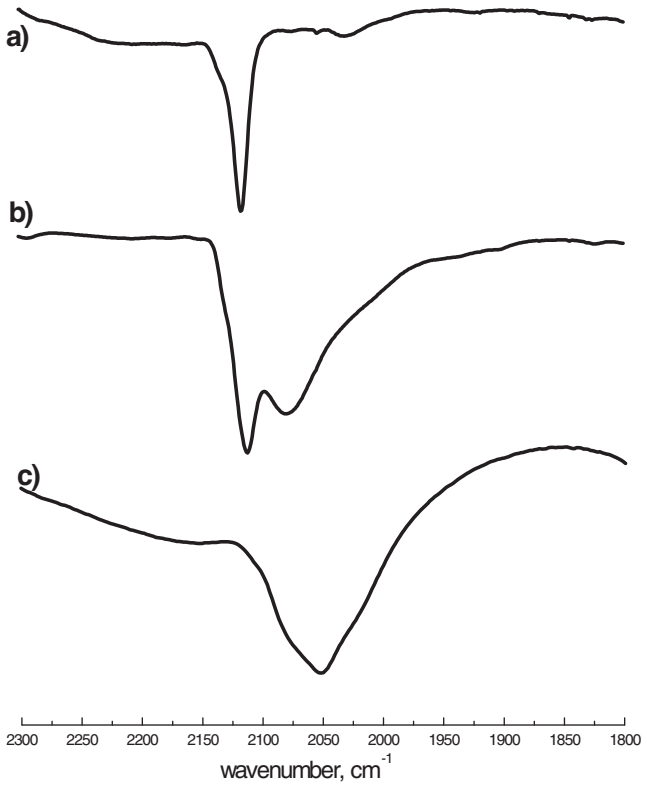

Fig. 6. Infrared spectra of **1** (a) and **4** (b) in methanol and **4** in water (c).

The energy and shape of the cyanide stretches of **4** in water (Fig. 6c), are very different from the pattern observed for the other systems. Instead of a set of band around 2100 cm^{-1}, a series of overlapping bands centered at 2050 cm^{-1} are observed. This energy value is typical for a hexacyanoferrate(II) moiety and confirms the presence of the Ru(III)–Fe(II) isomer in this solvent.

3.5. Analysis of the MM′CT band

We performed a two-state Mulliken–Hush treatment [32] on the MM′CT band of this family of complexes We followed the same treatment as in Ref. [33], where a detailed explanation of the theoretical background of the model as well as the fitting procedure can be found. The model describes the two diabatic states involved

Table 3
Absorption maxima and parameters obtained from the electronic spectra of the complexes studied in this work.

Complex	Solvent	ν_{MMCT} (10^3 cm^{-1})	ΔG^0 (10^3 cm^{-1})	λ_1/λ_2 (10^3 cm^{-1})	H_{12} (10^3 cm^{-1})[a]	$100C_1^2\|100C_2^2$	H_{12}[a] (10^3 cm^{-1})[b]
1	DMA[b]	17.0	14.0	1.6/3.6	0.8	99.7|0.3	0.9
	acetonitrile	15.6	12.5		0.9	99.7|0.3	1.0
	ethanol	13.7	10.5		1.1	99.4|0.6	1.1
	methanol	12.5	9.3		1.1	99.3|0.7	1.1
	water	8.8	5.8		1.3	98.2|1.8	1.3
2	DMA	16.7	13.9	1.3/3.4	0.9	99.8|0.2	0.8
	acetonitrile	15.2	12.3		0.9	99.7|0.3	0.8
	ethanol	13.2	10.3		1.1	99.4|0.6	1.0
	methanol	12.2	9.1		1.1	99.2|0.8	1.0
	water	8.3	5.6		1.2	98.0|2.0	1.1
3	DMA	15.8	11.8	2.6/3.4	0.9	99.7|0.3	0.9
	acetonitrile	14.2	10.1		1.0	99.5|0.5	1.0
	ethanol	12.0	8.2		1.2	99.1|0.9	1.1
	methanol	11.0	7.0		1.1	99.2|0.8	1.1
4	DMA	12.4	9.6	1.3/3.4	0.8	99.5|0.5	0.9
	acetonitrile	11.0	8.2		0.8	99.4|0.6	0.9
	methanol	7.2	4.7		1.1	98.2|1.8	1.0

[a] H_{12} calculated using $H_{12} = (0.0205/r_{12})[\varepsilon_{max}\,\Delta\nu_{1/2}\nu_{max}]^{1/2}$.
[b] DMA = dimethylacethamide.

in the transition as two quadratic functions connected by an electron transfer coordinate. The main parameters are ΔG^0, the relative free enthalpy between the states, λ_1 and λ_2, the Marcus reorganization energies of each surface and H_{12}, which represents the electronic interaction between the states that leads to mixing of the diabatic surfaces to yield the adiabatic potential curves. Additionally, we considered μ^D, the diabatic transition moment, as equal to $-er$, where the r value was fixed at the experimental Fe–Ru geometrical distance found in related complexes (5 Å). According to Stark spectroscopy measurements in some mixed-valent cyanide-bridged dinuclear complexes, the effective one-electron-transfer distance is smaller than the geometrical separation [4], but the difference should not be large if the mixing between fragments is not very high.

Even though each parameter could be treated independently, it is more informative to impose some restrictions. We kept λ_1 and λ_2 fixed for the same complex in different solvents as we expected a stronger dependence of the reorganization energy on the structure of the complex compared to the effect of the solvent. This behavior has been previously observed for the related trinuclear complexes in Ref. [33] and is probably related to the diminished role of the solvent in the reorganization energy due to its specific interaction with the terminal cyanides in both, the ground and the excited state. The final optimized parameters obtained from this fitting procedure are listed in Table 3. The simulated spectra of **1** in different solvents are displayed in Fig. 7 showing that the band shape of the experimental CT is well reproduced (for the remaining spectra see Fig. S2). The exception is again the spectrum of **4** in water which could not be fitted using the same set of parameters, which is not surprising considering the different nature of this transition.

The results are in line with the obtained for the related trinuclear complexes trans-$[L_4Ru\{(\mu\text{-}NC)Fe(CN)_5\}_2]^{4-}$. The diabatic free-energy varies with nature of coordination sphere of the ruthenium and with the acceptor properties of the solvent. The reorganization energy of the ground state is significantly smaller due to stabilizing effect of the solvent interaction at the coordinates of the electronic isomer. The values obtained for H_{12} are similar to the ones calculated using the Mulliken–Hush expression [34–37] (Table 3) and are comparable to the values reported for other cyanide-bridged dinuclear systems [4,9,38,39]. A moderate increment in solvents with a larger acceptor capability is observed.

As expected, all the systems analyzed show a low degree of mixing, with the Ru(II)–Fe(III) form as the dominant form with only a minor contribution from the Ru(III)–Fe(II) configuration

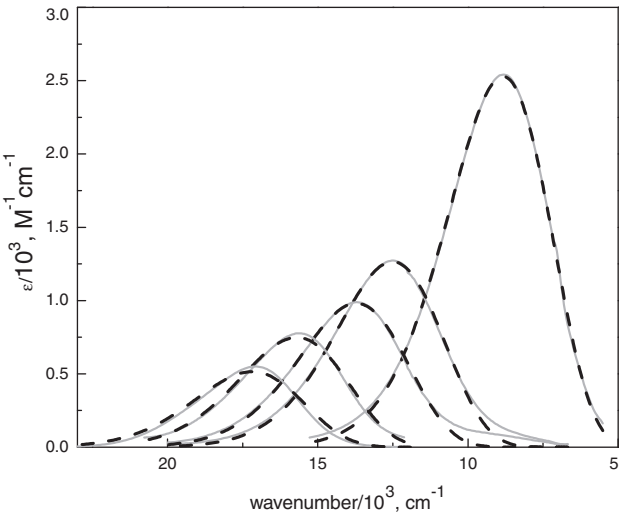

Fig. 7. Experimental (solid line) and simulated (dotted line) MM′CT bands of comples **1** in DMA, acetonitrile, ethanol, methanol and water.

(at most 2%). The trend observed for these complexes predicts a small, but positive value for the diabatic energy of **4** in water, *i.e.* the stable configuration should be the Ru(II)–Fe(III) isomer. Surprisingly the Ru(III)–Fe(II) configuration is observed. Probably the more favorable terminal cyanide-water interaction in the $Fe^{II}(CN)_5$ fragment favors the Ru(III)–Fe(II) isomer and prevents the existence of a Ru(II)–Fe(III) system with a small ΔG^0 between the states where some electronic delocalization could have been expected. There are reports of other mixed valence systems with terminal cyanides that show very little interaction in water [40], but in those cases a mismatch between the energy of the vacant orbitals of the pyrazine bridge and the dπ orbitals of the metal ions has been suggested as the explanation for this behavior [41].

4. Conclusions

We have explored the properties of the family cyanide bridged mixed valence dinuclear complexes. The difference in energy between these fragments can be tuned by variation of donor properties of the ligands around the ruthenium and the acceptor

properties of the solvent. Introduction of the very basic ligand dmap allows us to diminish the energy difference between the fragments, which results in a better mixing between the dπ orbitals. The observation of the transition from class II to class III in system 4 was precluded by the strong interaction of the water with the terminal cyanides, which traps the system in its Ru(III)–Fe(II) isomer, a result that emphasizes the ability of solvent interactions to localize a mixed valence system.

Acknowledgments

The authors thank the University of Buenos Aires and the Consejo Nacional de Investigaciones Científicas y Técnicas (CONICET) for economic funding. P. A. and L. B. V are members of the scientific staff of CONICET. M.B.R. is a graduate fellow of CONICET.

Appendix A. Supplementary material

Supplementary data associated with this article can be found, in the online version, at doi:10.1016/j.ica.2011.03.032.

References

[1] P. Day, N.S. Hush, R.J.H. Clark, Philos. Trans. R. Soc. A 366 (2008) 5.
[2] M.B. Robin, P. Day, Adv. Inorg. Chem. Radiochem. 10 (1967) 247.
[3] K.D. Demadis, C.M. Hartshorn, T.J. Meyer, Chem. Rev. 101 (2001) 2655.
[4] F.W. Vance, R.V. Slone, C.L. Stern, J.T. Hupp, Chem. Phys. 253 (2000) 313.
[5] H. Vahrenkamp, A. Geiss, G.N. Richardson, J. Chem. Soc. Dalton Trans. (1997) 3643.
[6] T.L. Sheng, H. Vahrenkamp, Eur. J. Inorg. Chem. (2004) 1198.
[7] G. Rogez, E. Riviere, T. Mallah, C.R. Chim. 6 (2003) 283.
[8] B.W. Pfennig, V.A. Fritchman, K.A. Hayman, Inorg. Chem. 40 (2001) 255.
[9] A.V. Macatangay, J.F. Endicott, Inorg. Chem. 39 (2000) 437.
[10] K.R. Dunbar, R.A. Heintz, Progress in Inorganic Chemistry, vol. 45, 1997, p. 283.
[11] P.V. Bernhardt, F. Bozoglian, B.P. Macpherson, M. Martinez, Coord. Chem. Rev. 249 (2005) 1902.
[12] C.P. Berlinguette, A. Dragulescu-Andrasi, A. Sieber, H.U. Gudel, C. Achim, K.R. Dunbar, J. Am. Chem. Soc. 127 (2005) 6766.
[13] L.M. Baraldo, P. Forlano, A.R. Parise, L.D. Slep, J.A. Olabe, Coord. Chem. Rev. 219 (2001) 881.
[14] C.J. Adams, N.G. Connelly, N.J. Goodwin, O.D. Hayward, A.G. Orpen, A.J. Wood, Dalton Trans. (2006) 3584.
[15] P. Albores, L.D. Slep, T. Weyhermuller, L.M. Baraldo, Inorg. Chem. 43 (2004) 6762.
[16] M.B. Rossi, K.A. Abboud, P. Albores, L.M. Baraldo, Eur. J. Inorg. Chem. (2010) 5613.
[17] M.B. Rossi, O.E. Piro, E.E. Castellano, P. Albores, L.M. Baraldo, Inorg. Chem. 47 (2008) 2416.
[18] B.J. Coe, T.J. Meyer, P.S. White, Inorg. Chem. 34 (1995) 593.
[19] W.L.F. Armarego, D.D. Perrin, Purification of Laboratory Chemicals, 4th ed., Butterworth-Heinemann, Oxford, UK, 1996.
[20] I. Noviandri, K.N. Brown, D.S. Fleming, P.T. Gulyas, P.A. Lay, A.F. Masters, L. Phillips, J. Phys. Chem. B 103 (1999) 6713.
[21] W. Kaim, J. Fiedler, Chem. Soc. Rev. 38 (2009) 3373.
[22] C.J. Timpson, C.A. Bignozzi, B.P. Sullivan, E.M. Kober, T.J. Meyer, J. Phys. Chem. 100 (1996) 2915.
[23] C.R. Johnson, W.W. Henderson, R.E. Shepherd, Inorg. Chem. 23 (1984) 2754.
[24] R.E. Shepherd, M.F. Hoq, N. Hoblack, C.R. Johnson, Inorg. Chem. 23 (1984) 3249.
[25] A. Burewicz, A. Haim, Inorg. Chem. 27 (1988) 1611.
[26] S. Siddiqui, W.W. Henderson, R.E. Shepherd, Inorg. Chem. 26 (1987) 3101.
[27] E.H. Cutin, N.E. Katz, Polyhedron 12 (1993) 955.
[28] W.M. Laidlaw, R.G. Denning, J. Chem. Soc. Dalton Trans. (1994) 1987.
[29] C.J. Timpson, Ph.D. Dissertation, University of North Carolina, Chapel Hill, North Carolina, USA, 1995.
[30] F. Roncaroli, L.M. Baraldo, L.D. Slep, J.A. Olabe, Inorg. Chem. 41 (2002) 1930.
[31] R.C. Rocha, A.P. Shreve, Inorg. Chem. 43 (2004) 2231.
[32] R.J. Cave, M.D. Newton, Chem. Phys. Lett. 249 (1996) 15.
[33] P. Albores, M.B. Rossi, L.M. Baraldo, L.D. Slep, Inorg. Chem. 45 (2006) 10595.
[34] R.S. Mulliken, J. Am. Chem. Soc. 74 (1952) 811.
[35] N.S. Hush, Prog. Inorg. Chem. 8 (1967) 391.
[36] N.S. Hush, Electrochim. Acta 13 (1968) 1005.
[37] C. Creutz, M.D. Newton, N. Sutin, J. Photochem. Photobiol. A Chem. 82 (1994) 47.
[38] F. Scandola, R. Argazzi, C.A. Bignozzi, C. Chiorboli, M.T. Indelli, M.A. Rampi, Coord. Chem. Rev. 125 (1993) 283.
[39] M.A. Watzky, A.V. Macatangay, R.A. VanCamp, S.E. Mazzetto, X.Q. Song, J.F. Endicott, T. Buranda, J. Phys. Chem. A 101 (1997) 8441.
[40] M. Ketterle, W. Kaim, J.A. Olabe, A.R. Parise, J. Fiedler, Inorg. Chim. Acta 291 (1999) 66.
[41] W. Kaim, A. Klein, M. Glockle, Acc. Chem. Res. 33 (2000) 755.